Simulation of realistic infrared texture of aeolian sand ripples

LIU Qian[1,2,3,4], ZHU Feng[1, 3,4], LONG Xiao-wei[5], HAO Ying-ming[1, 3,4], FU Shuang-fei[1, 3,4]
1 Shenyang Institute of Automation, Chinese Academy of Sciences, Shenyang, China
2 Graduate School of the Chinese Academy of Sciences, Beijing, China
3 Key Laboratory of Opto-Electronics Information Processing, Chinese Academy of Sciences, Shenyang, China
4 Key Laboratory of Image Understanding and Computer Vision, Liaoning Province, Shenyang
5 Military Representative Office of Air Force in Jiangxi Area, Nanchang, China
E-mail: {liuqian, fzhu, ymhao}@sia.cn

ABSTRACT

Texture is of vital importance when rendering realistic infrared images. Traditional attempts to simulate infrared textures often suffer from insufficient realism seen in actual infrared images. This paper presents a synthesis model for generating infrared texture of aeolian sand ripples. By integration of physical radiation model and texture structure model, sources of variability that causes IR texture are modeled. The physical radiation model takes into account geometrical, thermodynamic and meteorological parameters and calculates the thermal radiation distribution of different surface slopes. The texture structure model is introduced based on natural landscape features to simulate spatial distribution patterns of aeolian sand ripples. Simulation results are indicative of good performance of the proposed method to simulate radiometrically-correct yet visually-appealing infrared textures.

Keywords: infrared texture; realistic simulation; thermal radiation; texture structure

1. INTRODUCTION

Thermal infrared (TIR) imaging can be found widespread applications in such fields as remote sensing, agriculture, and military because of the incredible ability at anti-jamming in all-weather operations. The goal of infrared (IR) imagery simulation is to provide a practical alternative to the often expensive cost and staggering effort required to collect actual data.

As texture is the decisive factor in representation and recognition of natural objects, researchers of industry and academic alike have attached much importance to rendering visually realistic IR texture in recent years. IR texture in this paper refers to the image's spatial and spectral in-class variability [1]. Generally, infrared texture can be generated in two ways: conversion from images of the visible (VIS) band, and model-based IR texture synthesis.

The conversion approach is based on rigorous segmentation of different material regions of a VIS image. Each material is attributed optical and thermodynamic properties (absorptive, emissive, thermal conductivity, thermal capacity, et al). By using thermal models, surface temperatures for each material under various conditions are predicted, and thermal radiations are calculated. The gray scale representation of TIR radiation is obtained by mapping different IR characteristics to corresponding material regions. An obvious drawback emerges when large-scale, continuous regions with simplex material composition exist in the simulated scene. The conversion approach often suffers from a lack of realism because homogenous regions are mapped uniform gray level, thus simulated results fail to preserve the natural details seen in actual TIR images.

Foundation: This work is supported by Science Foundation of The Chinese Academy of Sciences, No. CXJJ-11-S100

Corresponding author: Liu Qian. E-mail: liuqian@sia.cn

International Symposium on Photoelectronic Detection and Imaging 2011: Advances in Infrared Imaging and Applications, Jeffery J. Puschell, Junhao Chu, Haimei Gong, Jin Lu, Eds., Proc. of SPIE Vol. 8193, 819308 · © 2011 SPIE · CCC code: 0277-786X/11/$18 · doi: 10.1117/12.896415

In 1994, Gambotto [2] proposed an analysis/synthesis simulation procedure. Specific algorithms were developed to extract texture signal from VIS images based on the assumption that texture resulted from small changes in region properties such as: reflective or thermal properties and surface orientation, and texture signal was dependent on average luminance and contrast of the region. However, texture signal derived in this method is unstable as situation (such as weather conditions, time and view angle) changes. In 2003, Shao et al. [3] presented an image synthesis method on the premise that textures of different spectral bands had similar gray distributions. Then texture mask taken from a VIS image is regarded as the gray level fluctuation. IR textures are synthesized by introduction of the texture mask. In fact, simply using texture mask of visible images to generate infrared texture is unreliable most of the time, because visible texture and infrared texture have essential differences in origin: visible textures are caused by spectral reflectance changes, while infrared textures are reflection of thermal radiation variances. Recently, infrared textures are generated from VIS images in order to augment fidelity [4][5]. By considering atmosphere attenuation, blurring effect and sensor noise, texture details are added simply through normal distribution random function in image plane. In spite of all these efforts in conversion of VIS images to infrared textures, natural textures are not synthesized adequately.

Model based texture synthesis uses mathematical models to describe and generate textures. Markov Random Field (MRF) [6][7][8] is deemed to be the most successful texture model, and several other models (GLC [9], SAR [10], CM) and algorithms also found widespread applications. These models are insufficient in practical use in two aspects. On the one hand, for different types of textures, the model parameters need to be adjusted repeatedly; sometimes it is even impossible to find suitable parameters. On the other hand, synthesizing textures by feature matching (such as pix-based and patch-based texture synthesis) is greatly subjected to the complexity of texture samples. To sum up, current methods are insufficient to deal with arbitrary textures, especially natural textures.

Aeolian sand ripples are the smallest sand pattern formed by wind and also basic structure of desert landscape. Traditional approaches cannot sufficiently create realistic infrared textures. In order to improve upon existing texture generation methods, a novel IR texture synthesis method consisting of a physical radiation model and a texture structure model is proposed. The remainder of this paper is organized as follows. In section 2, the physical radiation model is constructed by incorporation of geometrical, thermodynamic and meteorological parameters. The texture structure model is introduced in section 3 based on natural relief features to add realism to IR textures. Section 4 presents the texture synthesis process, and section 5 shows the simulation results of aeolian sand ripples. Conclusions and discussions are given in section 6.

2. PHYSICAL RADIATION MODEL

Since materials show both geometrical and thermal variances [11], models accommodating both geometric and thermodynamic inhomogeneities would have good performance in realistic IR simulation. The physical radiation model is an energy conservation process dependent on heat exchanges with the environment and on the geometrical and thermo-dynamical properties of surface materials.

2.1 Geometry Model

Surface geometry modeling is very important in simulation because absorptive and reflective irradiance by the sun and sky is sensitive to geometrical properties. For large-scale landscapes, accurate geometry modeling can be huge workload. In this paper, a simplified geometry model is used.

Natural aeolian sand ripples are composed of convex windward slopes and concave leeward slopes [12]. Fig.1 shows the cross section of aeolian sand ripples: Fig.1 (a) is the cross section of real sand ripples; Fig.1 (b) is the simplified geometrical model. In Fig.1, an east wind causes a flat eastward/windward slope and a steep westward/leeward slope. We use the surface roughness model proposed by Torrance and Sparrow [13] that assumes the land surface to be consisting of asymmetric V-cavities with upper edges in the same plane [14]. It can be seen from Fig.1 that the simplified geometrical model is much closer to the real one.

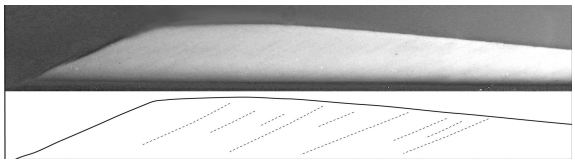

(a) cross section of real sand ripple

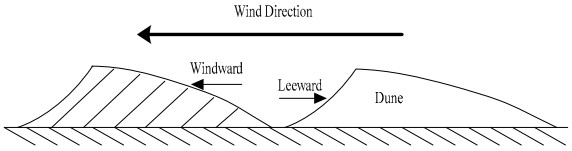

(b) simplified geometrical model for cross section of sand ripple

Figure 1. Cross section of aeolian sand ripples

In this paper, the surface geometry is described in terms of surface slope θ and azimuth angle ϕ. The geometrical parameters for windward (eastward) and leeward (westward) slopes are (θ_e, ϕ_e) and (θ_w, ϕ_w):

$$28^\circ < \theta_w < 34^\circ \quad \phi_w = 90^\circ$$

$$1^\circ < \theta_e < 13^\circ \quad \phi_e = -90^\circ$$

Hesp et al. gave the slope angles along windward surface [15][16][17]: 9~18° for slope toe, 11~15° for medi-slope, 4~9° for upper slope, and 1° for dune crest. The slope angle of leeward surface has a gentle variance in comparison with windward surface. In this paper, the slope angles at several sample points (P1~ P7) are given, we utilize polynomial fitting algorithms to obtain the slope angles at every other position. In Fig.2, P1, P2, P3 represent slope toe, medi-slope and slope crest of leeward surface; P7, P6, P5, P4 represent slope toe, medi-slope, upper slope and slope crest of windward slope.

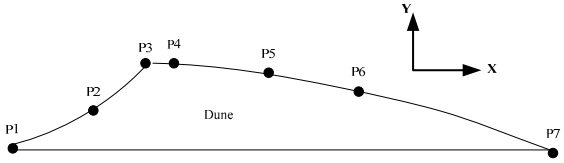

Figure 2. Sample points on simulated dune surface

The leeward slope can be expressed as:

$$y = mx^3 + mx^2 + px + q \tag{1}$$

where x and y represent the horizontal and vertical positions of surface sample point P; m, n, p, q are unknown parameters. Given the position of P1 and the slope angles at P1, P2, P3, the leeward slope can be easily solved. Similarly, the windward slope can be expressed as:

$$y = ax^4 + bx^3 + cx^2 + dx + e \tag{2}$$

Given the position of P7 and the slope angles at P4, P5, P6, P7, the unknown parameters a, b, c, d, e can also be solved. Assuming the x-coordinate of dune crest is 0, the dune cross section can be expressed by:

$$y = \begin{cases} mx^3 + mx^2 + px + q & x \le 0 \\ ax^4 + bx^3 + cx^2 + dx + e & x > 0 \end{cases} \tag{3}$$

The slope angle $slp(x)$ is surface gradient at (x, y), which can be determined by:

$$slp(x) = \arctan(\frac{dy}{dx}) \tag{4}$$

Surface points at the same slope are assigned the same azimuth angle: 90°for P1, P2, P3, and -90°for P4, P5, P6, P7.

2.2 Thermal Radiation Model

The prediction of surface temperature is handled by thermal radiation model that utilize material geometrical, thermodynamic, and meteorological parameters. The energy conservation on land surface is given by:

$$E_s + E_c + M_g + H + LE + G = 0 \tag{5}$$

where

E_s absorbed solar radiation

E_c downwelling radiation from the sky

M_g thermal radiation emitted by land surface

H sensible heat exchange

LE latent heat exchange

G conductive heat transfer

Surface temperature T is a nonlinear function of material properties, surface geometry, and meteorological conditions:

$$T = T(mat, geo, season, time, weather)$$

We use Newton-Raphson algorithm to solve surface temperature. Surface self-emission is calculated using Plank's law:

$$M(\lambda, T) = \varepsilon \cdot \int_{\lambda_1}^{\lambda_2} \frac{c_1}{\lambda^5} \exp\left(-\frac{c_2}{\lambda T}\right) d\lambda \tag{6}$$

where ε is the emissivity of surface material, $\lambda_1 \sim \lambda_2$ is the detected waveband, c_1 and c_2 are the radiation constants:

$$c_1 = 3.472 \times 10^{-16} W \cdot m^2, \; c_1 = 1.4388 \times 10^{-2} m \cdot K$$

The physical radiation model is foundation of generating a radiometrically-correct texture.

3. TEXTURE STRUCTURE MODEL

Texture is a major factor that impacts both the visual appearance and the overall scene statistics of imagery throughout the electromagnetic spectrum [18]. In this paper, we propose a texture structure model to add realism to infrared images.

3.1 Natural Features of Aeolian Sand Ripples

Fig.3 is VIS texture of aeolian and ripples. The morphological characteristics can be summarized as:

Figure 3. VIS texture of aeolian sand ripples

- A couple of waving curves (sand ridges) appear as evident texture elements in the image space of aeolian sand ripples.
- The spatial distribution of sand ridges exhibits some kind of periodicity.

Sand ridges are reflection of natural landscapes, and are common texture elements in both VIS and TIR bands. In this paper, we firstly propose to model sand ripples with B-spline fitting algorithms.

3.2 Texture Structure Model

Fig.4 shows the texture structure of aeolian sand ripples. Single sand ridge is represented by a waving curve.

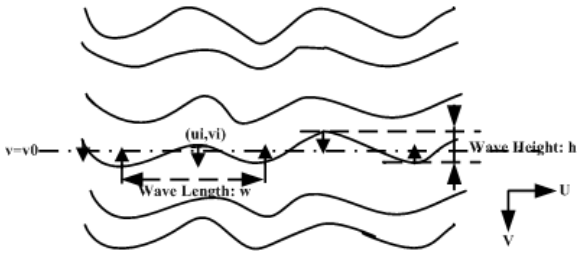

Figure 4. Texture structure of aeolian sand ripples

The smoothness and continuity of sand ridges is suitable for B-spline fitting. The texture structure can be expressed as:

$$B = \{B_k : k = 1, \cdots, n\} \tag{7}$$

where k is the sand ridge index, and n is the number of sand ridges in an image. Each sand ridge B_k is defined by several control points. The position of the ith control point (u_i, v_i) $(i = 0, \cdots, m-1)$ is determined by:

$$\begin{aligned} u_i &= i \cdot \frac{w}{2} + rand() \cdot \Delta w \\ v_i &= \begin{cases} v0 - \frac{h}{2} + rand() \cdot \Delta h & \mod(i,2) = 0 \\ v0 + \frac{h}{2} + rand() \cdot \Delta h & \mod(i,2) = 1 \end{cases} \end{aligned} \tag{8}$$

where m is the total number of control points per ridge; w and h are wave length and wave height respectively. $v = v0$ is the centerline of current sand ridge in V direction. $rand()$ is Gaussian random number ranging from 0 to 1; Δw is the wave length increment, Δh is the wave height increment:

$$\Delta w \in [-0.01Width, 0.01Width] \quad \Delta h \in [-0.01Height, 0.01Height]$$

where $Width \times Height$ is the image size. The two parameters should be controlled within a small range so that neighboring sand ridges will not intersect into each other.

In this paper, we use uniform cubic B-spline, assuming that control points are distributed with equa-distance in U direction. The kth sand ridge is fitted as the ensemble of $m-3$ spline curve fragments. Each fragment $S_j(t)$ is expressed by:

$$S_j(t) = \sum_{w=0}^{3} P_{j,w} b_w(t) \qquad t \in [0,1] \tag{9}$$

where $P_{j,w}$ is the ensemble of m control points, b_w is cubic B-spline basis:

$$\begin{aligned} b_0(t) &= \frac{1}{6}(-t^3 + 3t^2 - 3t + 1) \\ b_1(t) &= \frac{1}{6}(3t^3 - 6t^2 + 4) \\ b_2(t) &= \frac{1}{6}(-3t^3 + 3t^2 + 3t + 1) \\ b_3(t) &= \frac{1}{6}t^3 \end{aligned} \tag{10}$$

After the modeling of single sand ridge, the arrangement pattern of n sand ridges can be generated by adjusting the centerline $v = v0$. The proposed model is advantageous in simulating aeolian sand ripples with different spatial densities and directions by adjusting the wave length, wave height and direction.

4. INFRARED TEXTURE SYNTHESIS

IR textures of aeolian sand ripples are generated following three steps.

4.1 Surface Geometry Modeling

The goal of surface geometry modeling is to introduce surface geometrical variance into the IR radiation model. The slope angles of surface point change with its position. Points at the same slope share the same azimuth angle. The geometrical properties along sand dune are given in section 5.

4.2 IR Radiation Modeling

The hourly IR temperature and radiation are solved from physical radiation model. Among all the parameters that affect the surface radiation characteristics, material properties (solar absorptivity and thermal emissivity) are supposed to be homogenous in a diurnal cycle. We fix thermodynamic parameters in order to lower the remaining degrees of freedom in the IR radiation model.

Surface geometry is deemed as principle source of radiation variance, because it determines the effective angle of illumination by the sun and the amount of received diffuse irradiance from the sky and background. The predicted temperature and radiation are expected to have spatial variation from windward to leeward slopes. Moreover, surface temperature and radiation will change with meteorological conditions, so they will also present temporal variation.

To faithfully simulate the spatial distribution of IR radiation, temperature/radiation should be estimated on a per-pixel based. However, that will be notoriously time-consuming. In this paper, we choose several sample points representing different positions of surface slopes and calculate the hourly IR characteristics. Other surface points are fitted with these sample points.

4.3 IR Texture Simulation

Using the proposed method in section 3, the arrangement pattern of sand ridges is firstly drawn in image space. The two flanks of each sand ridge depict the leeward and windward slopes. The final infrared image is obtained by mapping the radiation distribution to corresponding positions in image space. We assume that gray level is proportion to radiation intensity, and adopt the following linear quantization formula:

$$Gray_i = [Gray_{\min} + \frac{M_i - M_{\min}}{M_{\max} - M_{\min}} \cdot (Gray_{\max} - Gray_{\min})] \tag{11}$$

where [] is round operation, $[Gray_{\min}, Gray_{\max}]$ is the gray range, typically $0 \sim 255$, $M_{\min}$ and $M_{\max}$ are minimum and maximum radiation along surface slopes, M_i is the calculated radiation at certain position. By (11), each position on the surface slope is assigned a gray level.

5. SIMULATION RESULTS

This section presents the results of using the above approach to simulate realistic IR texture of aeolian sand ripples. Firstly, surface geometry is modeled. Surface cross section fitted by polynomial fitting algorithms is expressed by:

$$y = \begin{cases} 0.00026x^3 + 0.0228x^2 + 0.6745x + 1.383 & x < 0 \\ -0.00014x^4 + 0.0034x^3 - 0.0313x^2 - 0.0175x + 1.383 & x \geq 0 \end{cases} \tag{12}$$

Slope angles are obtained from (4). Fig.5 shows slope angles from leeward to windward surfaces. Slope angles increase gently ($28^\circ \sim 34^\circ$) from leeward toe to dune crest, and decrease gradually ($13^\circ \sim 1^\circ$) from windward toe to crest.

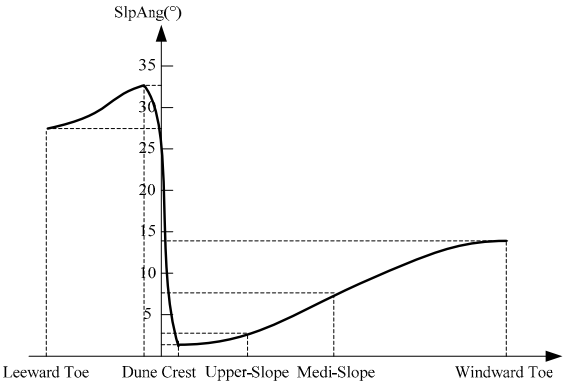

Figure 5. Slope angle vs. position plot along dune surface

Secondly, physical radiation model is used to compute temperature and radiation characteristics. The input parameters are listed in Table I.

TABLE I. PHYSICAL RADIATION MODEL INPUT PARAMETERS

Input Parameters	Values
Date	2010-10-29
Band	8~12 μm
Longitude	123.38°E
Latitude	41.8°N
Altitude	40m
Surface moisture content	0.36
Surface albedo	0.25
Surface emissivity	0.85
Heat conductivity	$0.66\ W/(m^2 \cdot K)$
Air density	$1.36\ Kg/m^3$
Air specific heat	$1006\ J/(Kg \cdot K)$
Leeward surface	Slope=28°~34° Azimuth=90°
Windward surface	Slope=1°~13° Azimuth=-90°

The actual radiation a thermal imager detects includes not only self-emitted radiation of object but also reflected and emitted radiations from the sun, sky and atmosphere. In this paper, the simulated waveband is LWIR (8~12 μm), where self-emitted irradiance is dominant. Average radiation of westward/leeward and eastward /windward slopes vs. time plots is shown in Fig.6. Eastward slope has higher radiation than westward slope from 7:00 am to 11:00, because eastward slope receives more solar insolation during the first few hours of sunrise. The intersection (crossover) of two curves occurs at 12:00, after that, the thermal radiations of westward slope exceed that of eastward slope from 13:00 am to 16:00, owing to more solar insolation in the east before sunset. The correlation curve is indicative of the decisive role of sun irradiation on surface thermal radiation during daytime.

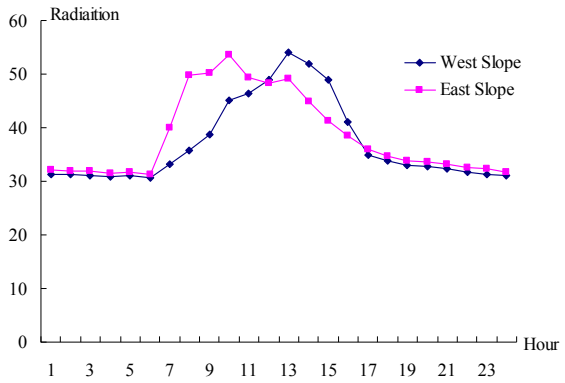

Figure 6. Average radiation vs. time plots for surface slopes

Fig.7 demonstrates the change of thermal radiation at different positions of surface slopes at 21:00 pm: sample points 1~11 on leeward slope and 12~22 on windward slope. Notice that IR radiation changes just in the opposite way as surface slope angle (see Fig.5): IR radiation decrease from leeward toe to dune crest, and increases from windward toe to crest. This is acceptable because diffuse irradiance from the sky is the main energy source at night. The reflected irradiance from the sky increases with slope angle increases, thus the absorptive irradiance decreases with increasing slope angle.

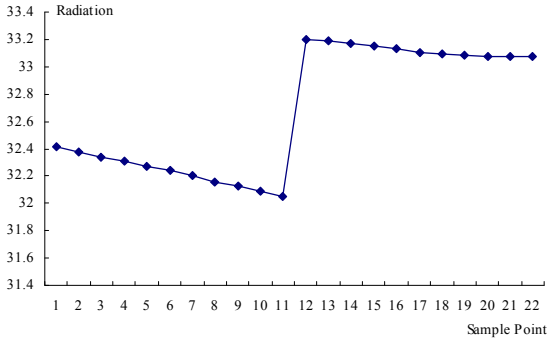

Figure 7. Self-emitted radiation at 21:00 pm on surface slopes

Thermal radiations are mapped to gray space using (11). The maximum and minimum radiations of the day-night cycle are:

$$M_{\max} = 54.03 W/m^2 \quad \text{(13:00 pm)}$$

$$M_{\min} = 30.48 W/m^2 \quad \text{(6:00 am)}$$

Finally, the proposed texture structure model is introduced to draw waving sand ridges in simulated textures. The thermal radiations of windward and leeward slopes are mapped to two flanks of sand ridges. Fig.8 shows the simulated infrared textures in the daytime (11:00) and at night (21:00). It is evident that average radiation determines the brightness of infrared textures. The number of control points and sand ridges determine the shape and spatial density of sand ripples.

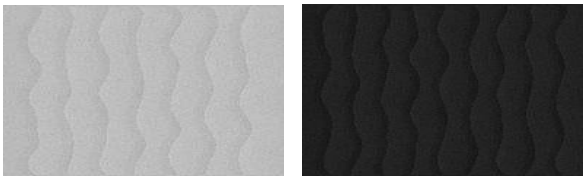

(a) IR texture at 11:00 am (b) IR texture at 21:00 pm

Figure 8. Simulated infrared textures of aeolian sand ripples

The texture parameters are listed in Table Ⅱ.

TABLE II. COMPARISON OF IR TEXTURE PARAMETERS

	Fig.8 (a)	**Fig.8 (b)**
Simulation Time	11:00 am	21:00 pm
Average Radiation	$\overline{M}_a = 47.73W/m^2$	$\overline{M}_b = 32.62W/m^2$
Average Intensity	$\overline{G}_a = 185$	$\overline{G}_b = 31$
Number of Sand Ridges	$n = 7$	$n = 9$
Control Points Per Sand Ridge	$m = 12$	$m = 12$

Strictly speaking, simulated IR textures should be compared with real IR imagery-the "correlating" screenshots taken from test simulation and from video recordings by a real sensor. There is however a lack of real imagery for aeolian sand ripples, which makes it hard to give quantitative assessment about how well the simulation results reflect real-world IR imagery. Under such circumstances, we have a qualitative evaluation of the realism of simulated IR texture by comparison with VIS texture. In Fig.8, windward/eastward slopes seem to be brighter than leeward/westward slopes, because surface temperature and radiation at simulated hours are higher. The spatial distribution of sand ripples in IR textures resembles the structural features in VIS images.

6. DISCUSSIONS AND CONCLUSIONS

Creating a visually-realistic yet radiometrically-accurate simulation of TIR imagery is a challenge in IR simulation. Previous attempts have suffered from insufficient realism when simulating natural textures. The proposed method aims to model sources of variability-surface geometry and induced variation in solar insolation and diffused sky irradiance. The main contribution includes but not limited to the texture structure model, which is applied to simulate the spatial pattern of aeolian sand ripples. Simulation results are indicative of good performance of the proposed method when reproducing the natural variability of aeolian sand ripples.

To summarize, the proposed method integrates basic principles of infrared radiation theory and a texture structure model to generate realistic IR textures. In fact, the texture simulation method should not be confined to aeolian sand ripples. Additional research could be undertaken by improvement of the texture structure model or utilization of thermal property variance to determine how well the framework of IR texture simulation may still perform.

REFERENCES

[1] Ward, J. T., "Realistic texture in simulated thermal infrared imagery," RIT Doctoral Paper, 25-30 (2008).

[2] Gambotto, J. P., "Combining image analysis and thermal models for infrared scene simulations," Proc. ICIP-94, 710-714 (1994).

[3] Shao, X. P., Zhang, J. Q. and Xu J., "Study of modeling natural infrared Textures," Journal of Xidian University, 30(5), 612-616 (2003).

[4] Shao, X. P., Wang, Z. Y., Zhou, T. F., et al., "Infrared image synthesis for bridges," Proc. SPIE 5405, 167-176 (2004).

[5] Chen, S. and Sun, J. Y., "IR scene simulation based on visual image," Infrared and Laser Engineering, 38(1), 23-30 (2009).

[6] Shao, X. P., Zhao X. M. and Zhang, J. Q., "Infrared texture simulation using Gaussian-Markov Random Fields," International Journal of Infrared and Millimeter Waves, 25(11), 1699-1710 (2004).

[7] Cross, G. R. and Jain, A. K., "Markov Random Filed texture models," IEEE Trans. Pattern Analysis and Machine Intelligence, 5, 25-39 (1983).

[8] Chellappa, R., Chatterjee, S. and Bagdazian, R., "Texture synthesis and compression using Gaussian-Markov Random Field Models," IEEE Trans. Systems, Man and Cybernetics, 15(2), 298-303 (1985).

[9] Bennett, J. and Khotanzad, A., "Modeling Textured images using Generalized Long Correlation Models," IEEE Trans. Pattern Analysis and Machine Intelligence, 20(12), 1365-1370 (1998).
[10] Mao, J. C. and Jain, A. K., "Texture classification and segmentation using multiresolution simultaneous autoregressive models," Pattern Recognition, 25(2), 173-188 (1992).
[11] Yu, W. J., Peng, Q. S., Tu, H. M., et al., "An infrared image synthesis model based on infrared physics and heat transfer," International Journal of Infrared and Millimeter Waves, 19(12), 1661-1669 (1998).
[12] Zheng, X. J., Bo, T. L., and Xie, Li., "DPTM simulation of aeolian sand ripple," Science in China Series G: Physics, Mechanics & Astronomy, 51(3), 328-336 (2008).
[13] Torrance, K. E. and Sparrow, E. M., "Theory for off-specular reflection from roughened surfaces," Journal of the Optical Society of America, 57(9), 1105-1114 (1967).
[14] Oren, M. and Nayar, S. K., "Generalization of Lambert's reflectance model," Proc. ACM. Computer Graphics and Interactive Techniques (SIGGRAPH 94), 239-246 (1994).
[15] Hesp, P. A. and Hastings, K., "Width, height and slope relationships and aerodynamic maintenance of barchans," Geomorphology, 22(2), 193-204 (1998).
[16] Sauermann, G., Rognon, P., Poliakov, A., et al., "The shape of the barchan dunes of Southern Morocco," Geomorphology, 36(1-2), 47-62 (2000).
[17] Livingstone, I. and Warren, A., [Aeolian Geomorphology-An Introduction], London: Addison Wesley Longman Limited, 211 (1996).
[18] Ward, J. T., Schott, J. R., Sanders, N. J., et al., "Driving realistic texture in simulated long-wave infrared imagery," IEEE Proc. Symp. Geoscience and Remote Sensing Symposium (IGARSS 08), 728-731 (2008).
[19] Sneh, A., "Permian dune patterns in Northwestern Europe challenged," Journal of Sedimentary Research, 58(1), 44-51 (1988).